The Secret Life of Collagen: Temporal Changes in Nanoscale Fibrillar Pre-Strain and Molecular Organization During Physiological Loading of Cartilage

*Sheetal R. Inamdar[1], David P. Knight[2], Nicholas J. Terrill[3], Angelo Karunaratne[4,†], Fernando Cacho-Nerin[3], Martin M. Knight[1] and Himadri S. Gupta[1]**

1. Institute of Bioengineering, School of Engineering and Materials Science, Queen Mary University of London, London

2. Bridge Cottage, Cwmyoy, Abergavenny, Wales

3. Diamond Light Source, Harwell Science and Innovation Campus, Harwell, Didcot

4. Department of Bioengineering, Imperial College London, London

Supplementary Information:

List of Supplementary Information Topics:

S.1: sGAG release and mechanical alterations on chondroitinase treatment.

S.2: Modelling SAXD intensity changes during stress relaxation in terms of fibrillar changes

S.3: Intrafibrillar molecular packing and fibril orientation during stress relaxation

S.1: sGAG release and mechanical alterations on chondroitinase treatment:

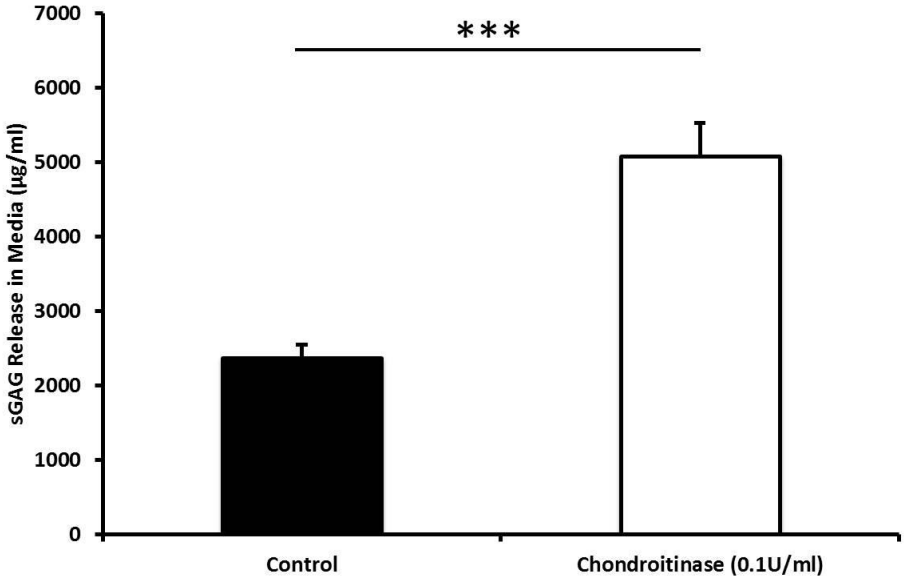

Figure S1: **Chondroitinase ABC treatment leads to increased sGAG release in treatment media**. Values represent mean values with error bars showing SEM for n = 12/group.

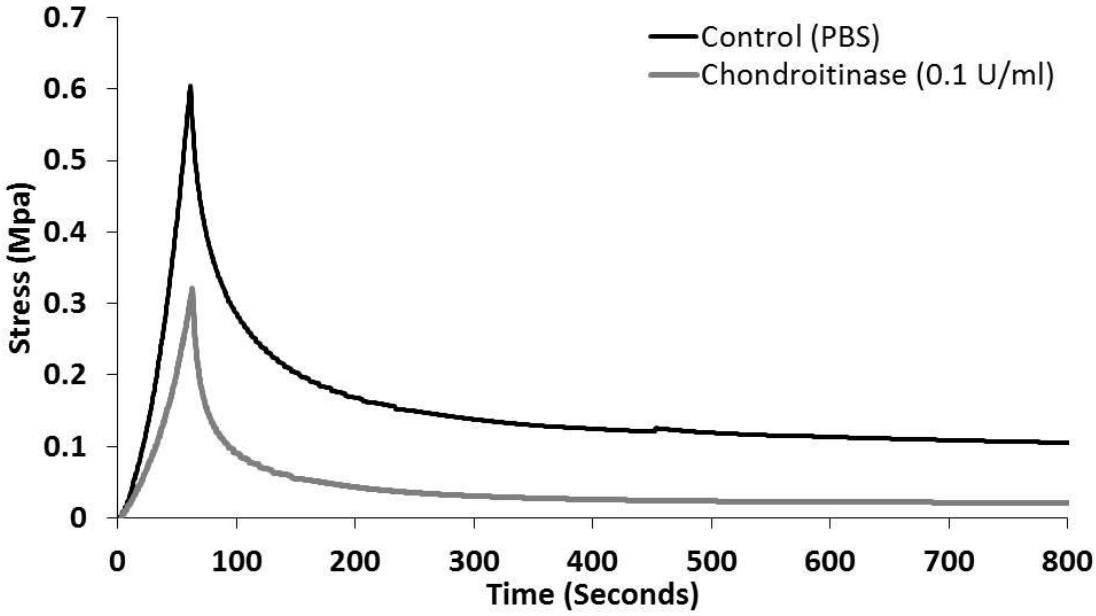

Figure S2: Chondroitinase ABC treatment leads to altered stress-relaxation response. Representative macro-scale stress response in compressed cartilage during relaxation (20% strain level loaded at a rate of 20%/min).

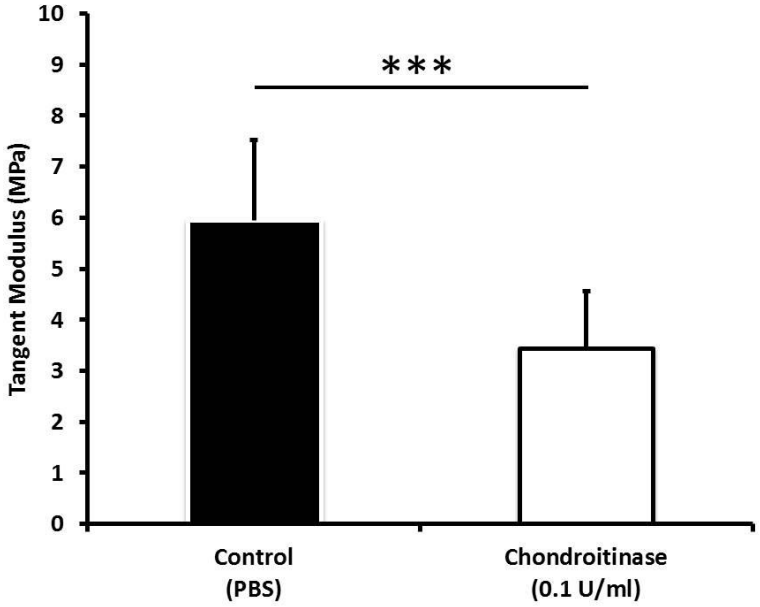

Figure S3: Chondroitinase ABC treatment leads to reduced tissue stiffness. Tangent modulus is significantly reduced when explants are treated with Chondroitinase ABC at 0.1U/ml. Tangent modulus was calculated from the linear region of the stress-strain curve. Values represent mean values with error bars showing SD for n = 9/group.

S.2: Modelling SAXD intensity changes during stress relaxation in terms of fibrillar changes

S.2A: Predictions of intensity ratio variation with changing O/D

Using the formulae for $\frac{I_7}{I_5}$ and $\frac{I_8}{I_5}$ derived from a step-function variation of axial electron density inside the collagen fibril (main text, **Materials and Methods**), the intensity ratios can be graphed as shown below. It is clear that there is a substantial sensitivity of peak intensity ratios to the exact value of O/D. In particular, in the region between O/D = 0.40 and O/D = 0.50, which is the value observed for collagen fibrils in a close-to-physiological condition[1] , the odd-order ratio $\frac{I_7}{I_5}$ and the even-order ratio $\frac{I_8}{I_5}$ vary in opposite directions.

[Supplementary information continues overleaf]

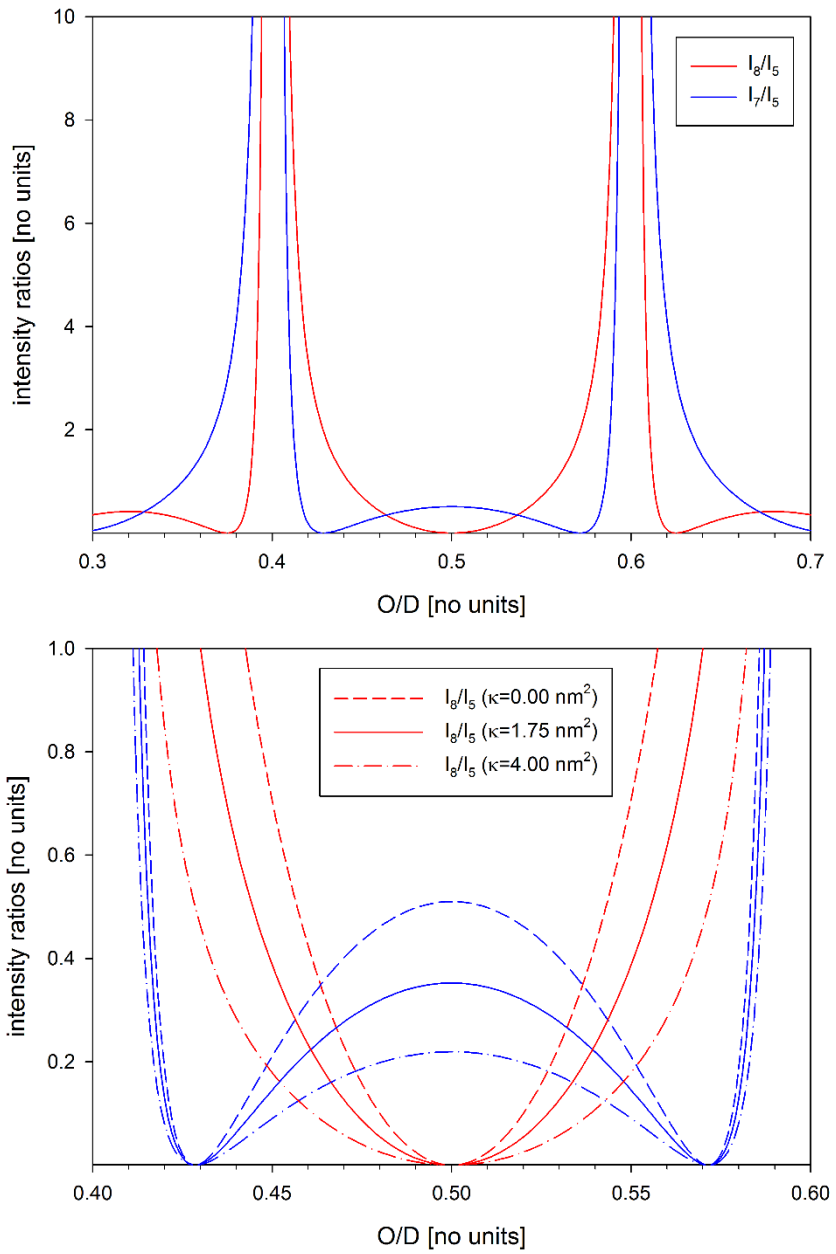

Figure S4: (a) Plot of $\frac{I_7}{I_5}$ (blue) and $\frac{I_8}{I_5}$ (red) with zero disorder over the O/D range from 0.3 to 0.7. Note how, over the range O/D ~ 0.45 – 0.50, $\frac{I_7}{I_5}$ increases while $\frac{I_8}{I_5}$ decreases. $\frac{I_8}{I_5}$ is zero at O/D = ½, as all even orders vanish at O/D = ½. (b) Plot of the variation of $\frac{I_7}{I_5}$ (blue) and $\frac{I_8}{I_5}$ (red) for three levels of disorder (κ = 0.00 nm^2 (dashed), 1.75 nm^2 (solid), and 4.00 nm^2 (dash-dot)) over a narrower O/D range from 0.4 to 0.6. The plot is an expanded version (in the abscissa and ordinate scales) of **Fig. 5D**.

[Supplementary information continues overleaf]

S.2B: Estimation of changed disorder and O/D during transient D-change:

We first describe qualitatively how the changes in intensity ratios can be interpreted in terms of disorder and O/D changes (part **S.2B1**) followed by a quantitative modelling of the variation of these parameters in part **S.2B2**.

S.2B1:

Estimate of initial disorder: From **Figure 5C** (main text), at the start of the dip in D-period (leftmost side of **Figure 5C**), $\frac{I_7}{I_5} \sim 0.25$ and $\frac{I_8}{I_5} \sim 0.15$. No mutually consistent solution for O/D can be found for these values for zero disorder ($\kappa = 0.00$ nm^2; **Figure S4**, dashed lines). By increasing κ, we find that at $\kappa \sim 1.75$ nm^2 (**Figure S4**, solid lines), $\frac{I_7}{I_5} \sim 0.25$ and $\frac{I_8}{I_5} \sim 0.15$ at O/D ~ 0.466, which is a mutually consistent solution, and provides an estimate of intrinsic disorder in the collagen fibrils before any load is applied. In the current discussion, all numerical values are approximate estimates from reading off the data plots and generated model curves, and are meant to demonstrate qualitative behaviours rather than numerically precise fits to data.

Increase of disorder: In the first stage (a→ b; **Figure 5C**), we observe a reduction of both $\frac{I_7}{I_5}$ to ~0.20 and $\frac{I_8}{I_5}$ to ~0.10. From **Figure S4**, it can be seen that such a change can be attained by keeping O/D fixed and increasing disorder from $\kappa \sim 1.75$ nm^2 to $\kappa \sim 4.00$ nm^2 (vertical downward arrows).

Reduction of O/D: In the second (middle) stage (b→ c; **Figure 5C**), $\frac{I_7}{I_5}$ decreases and $\frac{I_8}{I_5}$ increases till they both cross-over at ~ 0.15-0.16 at the point of minimum D. We can see from

Figs 5D and **S4** that such a behaviour can be modelled by keeping both $\frac{I_7}{I_5}$ and $\frac{I_8}{I_5}$ on their respective κ = 4.00 nm^2 curves, and reducing O/D till the curves intersect at ~0.457, which is also where both ratios are ~0.13.We can therefore see that the changes in peak intensity ratios during the minimum in fibrillar pre-strain in D can be explained by an initial increase in intrafibrillar disordering, followed by a reduction in O/D due axial movement of tropocollagen molecules, as shown schematically in **Figure 6** (main text; bottom row).

S.2B2:

The steps described above can be simulated, as guides to the eye rather than as a fit, by linear variations of the O/D fraction and the disorder term across the three stages, as follows.

(a → b): Denote the start and end time points of this segment to be t_1 (= 50 s) and t_2 (= 90 s). Then the rescaled time parameter can be defined as $\zeta_1 = \frac{t - t_1}{t_2 - t_1}$. With this, we have:

$$\kappa(\zeta_1) = \kappa_0 + \zeta_1(\kappa_1 - \kappa_0)$$

$$\left(\frac{I_7}{I_5}\right)_A(\zeta_1) = \left(\frac{I_7}{I_5}\right)_A(0)\exp\left(-24(\kappa(\zeta_1) - \kappa_0)\left(\frac{2\pi}{D}\right)^2\right)$$

$$\left(\frac{I_8}{I_5}\right)_A(\zeta_1) = \left(\frac{I_8}{I_5}\right)_A(0)\exp\left(-39(\kappa(\zeta_1) - \kappa_0)\left(\frac{2\pi}{D}\right)^2\right)$$

(b → c): Denote the start and end time points of this segment to be t_2 (= 90 s) and t_3 (= 110 s). Then the rescaled time parameter can be defined as $\zeta_2 = \frac{t - t_2}{t_3 - t_2}$. As over this segment, the overlap/D-period changes but the disorder remains constant, we have (abbreviating O/D as *f*):

$$f_B(t) = f_0 + \zeta_2(f_1 - f_0)$$

$$\left(\frac{I_7}{I_5}\right)_B(\zeta_2) = \left(\frac{5}{7}\right)^2\left(\frac{\sin(7\pi f_B(\zeta_2))}{\sin(5\pi f_B(\zeta_2))}\right)^2 \exp\left(-24\kappa_1\left(\frac{2\pi}{D}\right)^2\right)$$

$$\left(\frac{I_8}{I_5}\right)_B(\zeta_2) = \left(\frac{5}{8}\right)^2\left(\frac{\sin(8\pi f_B(\zeta_2))}{\sin(5\pi f_B(\zeta_2))}\right)^2 \exp\left(-39\kappa_1\left(\frac{2\pi}{D}\right)^2\right)$$

(c → d): Denote the start and end time points of this segment to be t_3 (= 110 s) and t_4 (= 150 s). If $\frac{I_8}{I_5} = \left(\frac{5}{8}\right)^2\left(\frac{\sin(8\pi f_1)}{\sin(5\pi f_1)}\right)^2 \exp\left(-39\kappa\left(\frac{2\pi}{D}\right)^2\right)$ is (approximately) constant, we can take the initial state as (κ_1, f_1), with

$$R_{8,5}^1 = \left(\frac{5}{8}\right)^2\left(\frac{\sin(8\pi f_1)}{\sin(5\pi f_1)}\right)^2 \exp\left(-39\kappa_1\left(\frac{2\pi}{D}\right)^2\right)$$

If we set $R_{8,5}^1$ as a constant ~0.11, then if the ratio f varies continuously from f_1 to f_2, with a variation parameter $\zeta_3 = \frac{t - t_3}{t_4 - t_3}$,

$$f_C(t) = f_1 + \zeta_3(f_0 - f_1)$$

with $0 \le \zeta_3 \le 1$, which leads to

$$\kappa(\zeta_3) = -\frac{1}{39}\left(\frac{D}{2\pi}\right)^2 \ln\left(\frac{64\sin^2(5\pi f_C(\zeta_3))}{25\sin^2(8\pi f_C(\zeta_3))} R_{8,5}^1\right)$$

whence one can construct the trajectory for $\frac{I_7}{I_5}$

$$\left(\frac{I_7}{I_5}\right)_C(\zeta_3) = \left(\frac{5}{7}\right)^2\left(\frac{\sin(7\pi f_C(\zeta_3))}{\sin(5\pi f_C(\zeta_3))}\right)^2 \exp\left(\frac{24}{39}\ln\left(\frac{64\sin^2(5\pi f_C(\zeta_3))}{25\sin^2(8\pi f_C(\zeta_3))} R_{8,5}^1\right)\right)$$

These two relations are used to complete the trajectories corresponding to the two closed curves in **Figure 5E**, are plotted below in **Fig S5**, and are reproduced in **Figure 5D** as dashed model estimates. Note that by keeping $\frac{I_8}{I_5}$ constant, the disorder κ decreases from κ=4.0 nm^2 but is still lower than the initial state (a; κ~1.75 nm^2) at the end (d; κ~2.8 nm^2), which is reflected in the levels after the dip being slightly lower than before the dip in **Fig. S4**.

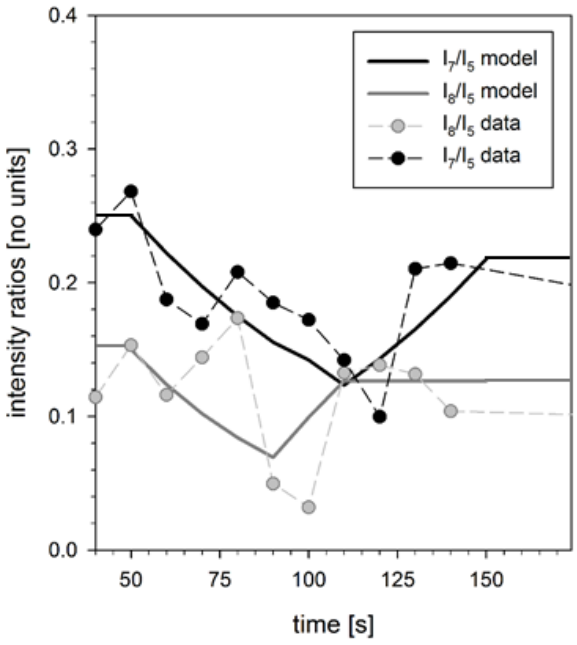

Fig S4: Intensity ratio variation for measured $\frac{I_7}{I_5}$ (black symbols/dashed line) and $\frac{I_8}{I_5}$ (grey symbols/dashed line) (data from main text **Fig. 5C**), together with model predictions for $\frac{I_7}{I_5}$ (solid black line) and $\frac{I_8}{I_5}$ (solid grey line)

Parameter variation in Figs. 5D and S5:

Stage	**O/D (*f*)** **[no units]**	**κ** **[nm^2]**	**I_7/I_5** **[no units]**	**I_8/I_5** **[no units]**
a→b	f_0	$\kappa_0 + \zeta_1(\kappa_1 - \kappa_0)$	$\left(\frac{I_7}{I_5}\right)_A(\zeta_1)$	$\left(\frac{I_8}{I_5}\right)_A(\zeta_1)$
b→c	$f_B(t) = f_0 + \zeta_2(f_1 - f_0)$	κ_1	$\left(\frac{I_7}{I_5}\right)_B(\zeta_2)$	$\left(\frac{I_8}{I_5}\right)_A(\zeta_2)$
c→d	$f_C(t) = f_1 + \zeta_3(f_0 - f_1)$	$\kappa(\zeta_3)$	$\left(\frac{I_7}{I_5}\right)_C(\zeta_3)$	$R^1_{8,5}$

Table S1: Summary of the variation of overlap/D-period, disorder parameter κ, and the intensity ratios I_7/I_5 and I_8/I_5 across the loop in **Figure 5E**. The different equations for each segment (subscripted A, B, C) are given in full in the text below; lack of space prevents reporting of the full equation in the Table above. The ζ-variables are dimensionless time-variables varying from 0 to 1. Numerical values f_0, f_1 are overlap/D-period values with f_0 = 0.466 and f_1 = 0.457. Disorder parameter values are κ_0 = 1.75 nm^2 and κ_1 = 4.00 nm^2. Initial values for I_7/I_5 and I_8/I_5 (at *a*) are $(I_7/I_5)_0 \sim 0.25$ and $(I_8/I_5)_0 \sim 0.15$ respectively.

[Supplementary information continues overleaf]

S.3: Intrafibrillar molecular packing and fibril orientation during stress relaxation

S.3A: Equatorial peak from intrafibrillar molecular packing:

Fig. S5 shows the equatorial SAXS profile before and after subtraction of a diffuse background term (modelled as an exponential decay). After background subtraction, the equatorial peak corresponding to the intermolecular spacing d_m is clearly visible. The data can be fitted to a Gaussian profile, as shown in Fig. S5B.

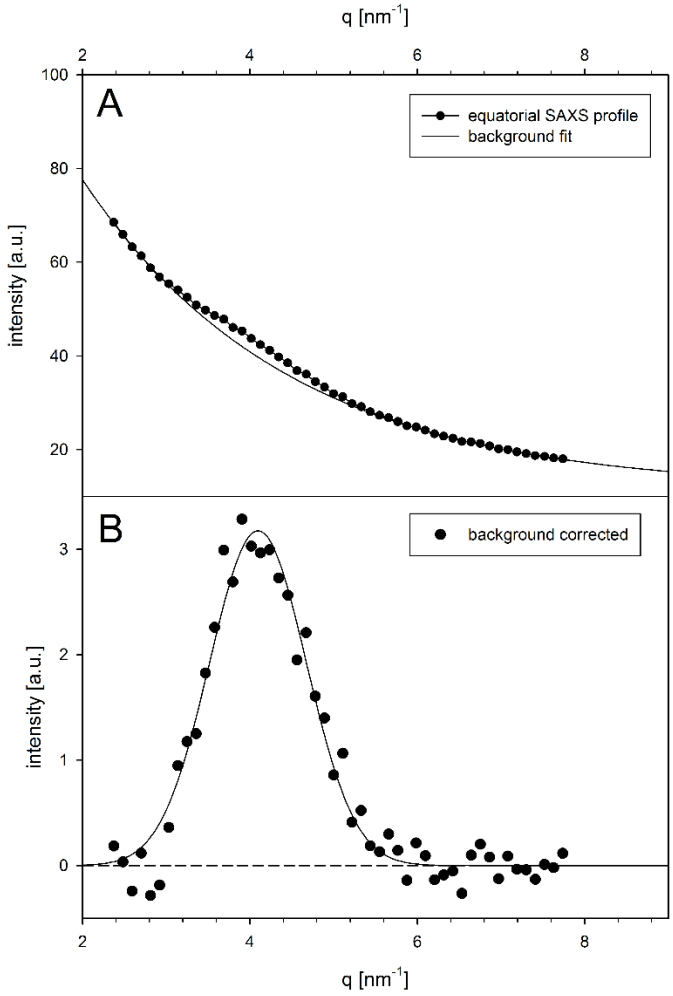

Fig S5: Equatorial SAXS intensity profile for cartilage (at zero strain), before (a) and after (b) subtraction of the diffuse SAXS scattering. After subtraction, the equatorial peak is observed at q ~ 4.0 nm^{-1} corresponding to d_m ~ 1.5 nm, characteristic of the lateral intermolecular spacing in hydrated collagen[2].

S3.B: Variation of intermolecular spacing and fibril orientation:

Fibril orientation parameters (angular position and width) are obtained from $I(\chi)$ profiles as described in the main text, ***Materials and Methods***. Intrafibrillar molecular spacing d_m is obtained as described above in ***S3.A***. The variation of these parameters is shown in **Fig. S6** below. **Figure S6A** clearly shows that no reduction of d_m from wet to dry values occurs around the point of pre-strain reduction. Lastly, **Figure S6B** shows no change in fibril orientation or width of the fibril angular distribution coinciding with the reduction in D-period.

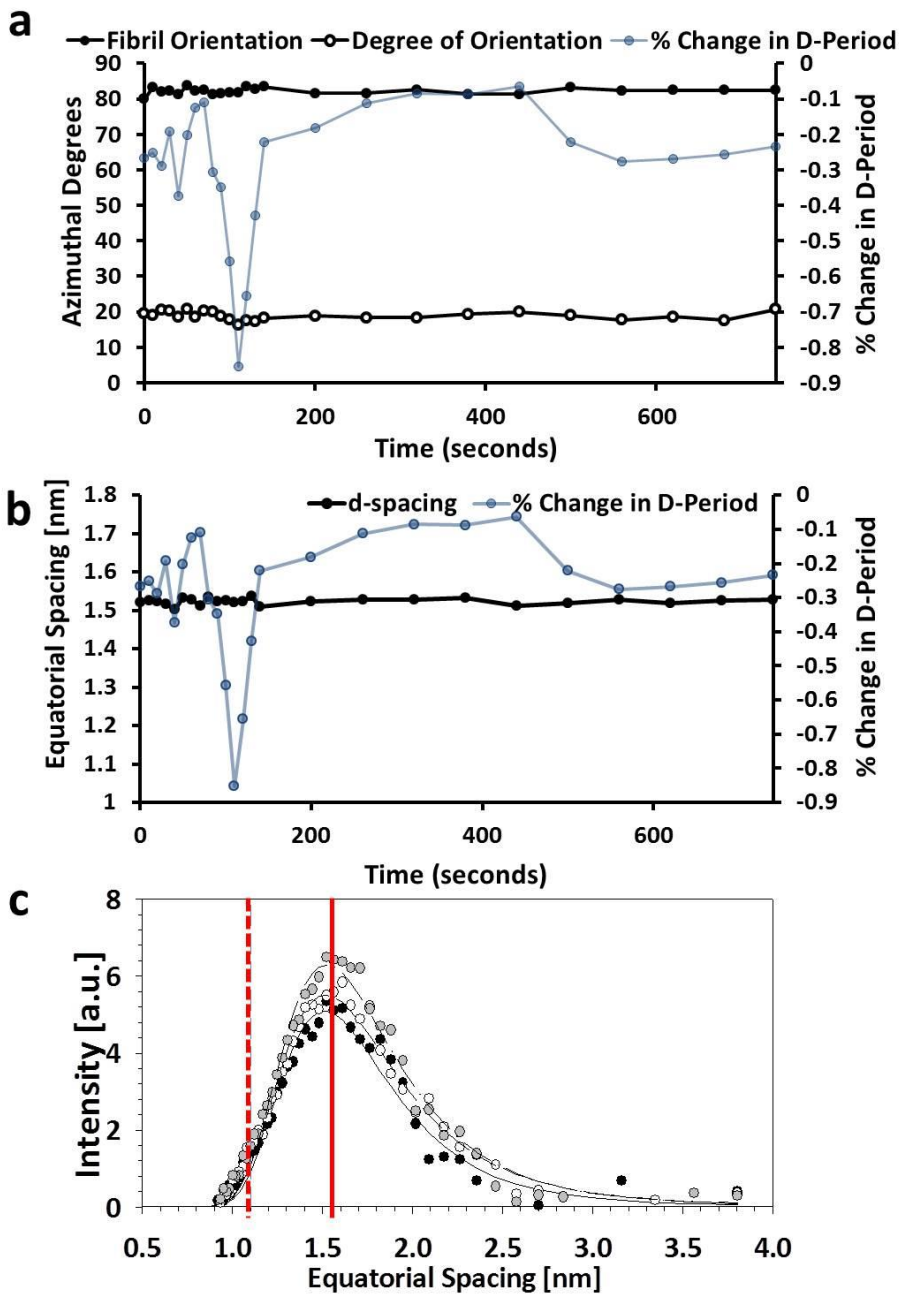

Fig S6: A) Average fibril orientation (filled symbols) and angular width of the fibril distribution (open symbols) show little change at the minimum in D (gray line), B) Intermolecular spacing d_m, calculated from the peak position of the equatorial SAXS peak, plotted together with the D-period (analogous to Fig. 5A-B in main text). C) Equatorial SAXS peak intensity profiles It is observed that d_m remains consistently at $d_m \sim 1.54$ nm (solid vertical line) characteristic of wet collagen[2] (dashed line shows the value for dry collagen $d_m \sim 1.1$ nm), and does not change during the transient change in D (gray line). Note that the equatorial SAXS profiles are plotted with the abscissa transformed from wavevector (in which domain the Gaussian fit was performed) to equatorial spacing by $d = 2\pi/q$.

Supplementary References:

1. Sasaki, N. & Odajima, S. Elongation Mechanisms of Collagen Fibrils and Force-Strain Relations of Tendons at Each Level of Structural Hierarchy. *J. Biomech.* **29,** 1131–1136 (1996).

2. Fratzl, P., Fratzl-Zelman, N. & Klaushofer K. Collagen Packing and Mineralization: An X-Ray Scattering Investigation of Turkey Leg Tendon. *Biophys. J.* **64,** 260–266 (1993).